ICOSSAR 2021
The 13th International Conference on Structural Safety and Reliability (ICOSSAR 2021), June 21-25, 2021, Shanghai, P.R. China
J. Li, Pol D. Spanos, J.B. Chen & Y.B. Peng (Eds)

Risk-Informed Decision-Making Framework for Emergency Response During Flooding

Pranavesh Panakkal[a], Jamie E. Padgett[b] and Philip Bedient[c]

[a]Department of Civil and Environmental Engineering, Rice University, Houston, Texas, USA, E-mail: pranavesh@rice.edu.
[b]Department of Civil and Environmental Engineering, Rice University, Houston, Texas, USA, E-mail: jamie.padgett@rice.edu.
[c]Department of Civil and Environmental Engineering, Rice University, Houston, Texas, USA, E-mail: bedient@rice.edu.

ABSTRACT: Real-time emergency response decision-making (DM) during flooding is a challenging problem. In contrast to the complexity of the problem, current DM frameworks are generally oversimplified and neglect the uncertainty, infrastructure performance and socio-demographics of the region. To address these limitations, this study poses a risk-informed DM framework that integrates situational awareness, exposure, vulnerability, and decision-making. First, real-time flood hazard information is obtained from a proven flood alert system. Next, the hazard data is coupled with performance models to estimate infrastructure performance at the component and network levels. Infrastructure performance is then placed in the context of socio-demographic data to inform decision making. In addition to proposing the integrated framework, this paper will present a case study application in Brays Bayou Watershed, Houston, Texas, USA. By quantifying risk and associated uncertainty, the framework can aid emergency managers seeking to identify high-risk locations and prioritize emergency response.

KEYWORDS: emergency response; flooding; decision making; situational awareness.

1 INTRODUCTION

Hurricane Harvey (2017), a slow-moving Category 4 hurricane, hovered near Houston dropping more than 1.3 meters of rain between 25 and 30 August 2017 (Zhang et al. 2018). The ensuing flood, impacted more than 270,000 houses and rendered more than 780,000 people in need of shelter (FEMA 2017a). More than 6400 people were rescued by Federal Emergency Management Agency (FEMA) Urban Search and Rescue teams alone (FEMA 2017b). At such a scale, emergency response operations require unprecedented inter-department collaboration, effective decision-making, and communication (Bharosa et al. 2010; Jiang & Yuan 2019). Decision-making is especially challenging due to the lack of situational awareness and limited resources. To elaborate, during a natural disaster such as floods, little information is often available on the flood extent and flood impact on infrastructure and community. In addition, the uncertainty associated with the available information and the dynamic nature of floods pose severe challenges to effective decision-making (Jiang & Yuan 2019). With a potential increase in future flood risk (Winsemius et al. 2016; Zscheischler et al. 2018), a robust situational awareness and decision-making framework is essential for enhancing community resilience.

Several studies in the domain of flood alert systems and structural health monitoring have attempted innovative frameworks to address the need for robust decision-making tools. Fang et al. (2008) proposed Rice/TMC flood alert system that uses real-time radar data and a precompiled floodplain map library to aid emergency response decision-making in the Texas Medical Center region, Houston, USA. More recently, Liu et al.'s (2018) flood prevention and emergency response system (FPERS) leverages historical and current forecast, remote sensing imageries, real-time monitoring of water levels from select gauges, and crowdsourcing for supporting decision making. Flood alert systems (Bedient et al. 2003; Demir & Krajewski 2013; Looper & Vieux 2012; Fang et al. 2008) provide information on the flood extents or streamflow and generally do not attempt to

characterize flood *impact* on infrastructure systems and communities.

While real-time information on flood extent is necessary, it alone is not sufficient for effective emergency response operations; characterizing infrastructure performance and its impact on the exposed communities are essential for decision-making. Real-time structural health monitoring (SHA) (Tokognon et al. 2017; Abdelgawad & Yelamarthi 2016) and Internet of Things (IoT) (Van Ackere et al. 2019; Perumal et al. 2015) can provide critical information and insights on the structural performance of infrastructure systems under stressors. Although SHA and IoT can assist in the decision-making process, the deployment, maintenance and operation of sensors can be prohibitively expensive at an optimum spatial density. Panakkal et al. (2019) proposed an alternative approach which couples a proven flood alert system with infrastructure performance models. Their model leveraged predelineated maps and inputs from a flood alert system to characterize flood impact on mobility. This approach could provide a cost-effective alternative for modeling infrastructure performance during flooding.

In addition to the limited consideration of infrastructure performance, current DM frameworks for floods generally lack in uncertainty quantification and support for probabilistic risk-based decision making (Jiang & Yuan 2019). This is concerning because emergency response decision-making is replete with uncertainties due to the paucity of real-time data, the dynamic nature of flooding, and the complex interaction between environmental forces, the built environment, and communities.

Similarly, existing frameworks provide limited consideration of the socio-demographics of the exposed population. This is contrary to the observations from several past studies that reported a disproportionate impact of flooding on vulnerable communities. For example, less expensive residential buildings may be more likely to experience greater relative damage than more expensive houses (Wing et al. 2020). Similarly, vulnerable populations are likely to see a higher mobility disruption and limited accessibility to health care facilities during flooding (Balomenos et al. 2019). Since the available resources and other socio-economic factors could influence evacuation, response, and recovery patterns during flooding (Rufat et al. 2015), a decision-making framework should explicitly consider the characteristics of the exposed population.

To address these identified limitations, this study proposes Risk-Informed Decision-making for Emergency Response (RIDER) framework. RIDER integrates near-real-time information on flooding, flood impact on different infrastructure systems, and characteristics of the exposed population. The hazard level is obtained from a real-time flood alert system such as Rice/TMC FAS. Consequences, defined here as the flood impact on infrastructure systems and communities, are modeled using predelineated deterministic and probabilistic maps. The 'risk measure' quantifies consequences given a hazard level. An example custom ‘risk measure’ would be "quantify the population in damaged buildings without either vehicles or access to evacuation routes." Precompiled maps enable RIDER to consider and propagate uncertainty without the computation and time cost associated with real-time execution of probabilistic analysis considering multiple variables and their interactions.

The rest of the paper is divided into three sections. Section 2 presents an overview of the RIDER framework. The components of RIDER and the methodology for developing the components are explained in detail. Next, Section 3 demonstrates a case study application of the RIDER framework to Brays Bayou watershed in Houston, Texas, USA. Finally, Section 4 lists conclusions and future research directions.

2 OVERVIEW OF RIDER FRAMEWORK

2.1 *Overview*

The RIDER framework proposed in this study leverages real-time flood inundation maps from Rice/TMC flood alert system. Rice/TMC FAS is selected due to two reasons: first, the FAS framework’s methodology utilizes precompiled maps that can overcome the computational expense required for real-time probabilistic analyses; second, the superior performance of Rice/TMC FAS was well documented during past flood events in the Brays Bayou watershed (Fang et al. 2011). Rice/TMC FAS consists of three main components. First, the data acquisition

module, acquires near-real time NEXRAD rainfall radar data at regular intervals. Second, flood plain map library (FPML), consists of a set of predelineated inundation maps. The FPML maps are generated using hydrological and hydraulic analysis after considering the characteristics of the watershed. Finally, a map selection algorithm processes the rainfall radar data and selects a flood inundation map that can closely represent the current inundation level in the watershed.

Following a structure similar to Rice/TMC FAS, the RIDER framework consists of four main components (Fig. 1). First, the Infrastructure Performance and Exposure Map Library (IPEML) consists of map groups quantifying flood impact on select infrastructure systems for each scenario in FPML. In addition, IPEML also contains maps quantifying the socio-demographics and social vulnerability of the exposed population. IPML can contain deterministic as well as probabilistic maps and are precompiled before the deployment of the RIDER platform. For each scenario map in Rice/TMC FAS FPML, there would be a set of linked IPEML maps. Second, the Data Acquisition module acquires the current scenario inundation map from Rice/TMC FAS. The third component, a map selection algorithm, selects pertinent maps from the IPEML for the current inundation scenario obtained from Rice/TMC FAS. Finally, the Decision-Making (DM) interface uses the identified maps from the map selection algorithm to answer queries from a decision-maker.

RIDER allows custom definitions of the 'risk measure' through queries. The 'risk measure' quantifies consequences given a hazard level. The hazard level is obtained from Rice/TMC FAS and a decision-maker can define the 'risk measure' based on available metrics from the IPEML maps linked to the current flood scenario. An example query would be "Identify regions with vulnerable populations (defined, for example, as population older than 60 years) in damaged buildings (defined, for example, as buildings with probability of building collapse greater than 50%) and limited access to evacuation routes." While running this query, the DM interface will perform a spatial query on the current maps from IPEML to identify the regions that match the provided criteria. A detailed description of the four components follows.

2.2 *Infrastructure Performance and Exposure Map Library (IPEML)*

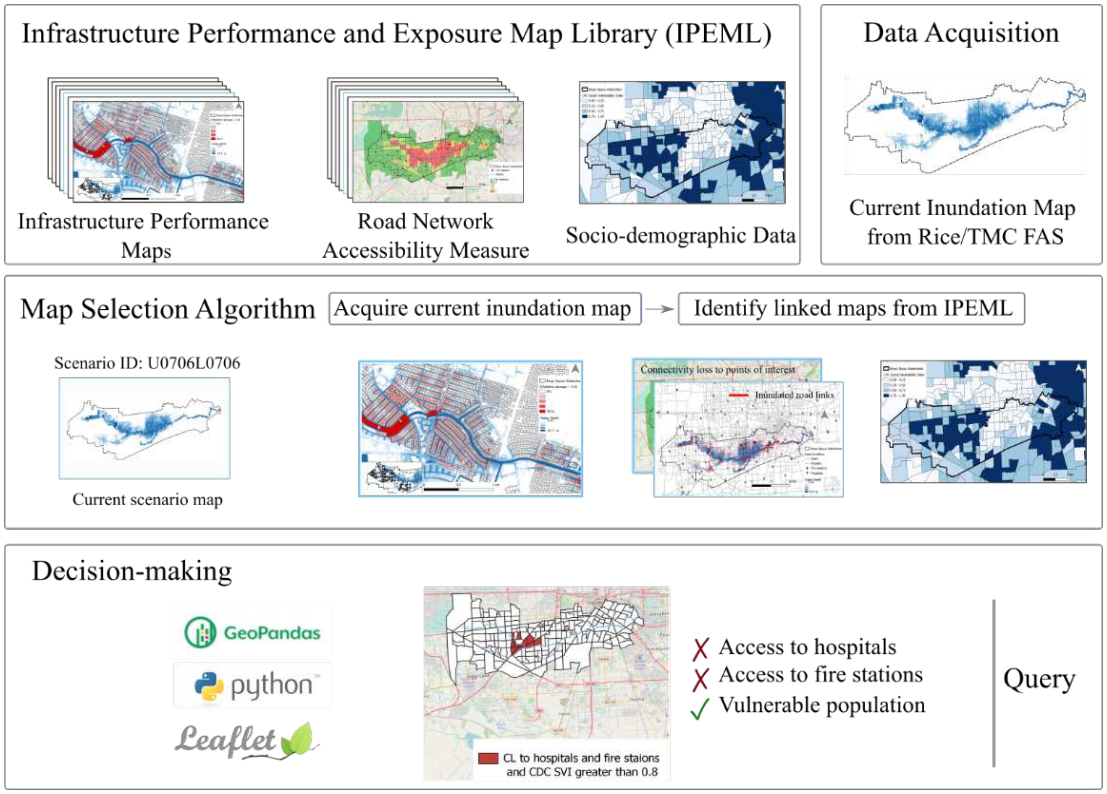

Figure 1. Overview of RIDER

IPEML consists of map groups characterizing infrastructure performance and socio-demographics of the exposed population. Each map group represents the state of an infrastructure system during flooding. Consequently, there can be one map group that captures the flood impact on the transportation network and another characterizing the flood impact on the residential buildings. Additional map groups can also capture the performance of critical structures such as chemical plants and industrial facilities. In addition, map groups can contain maps characterizing social-demographic characteristics of the study area.

Construction of map groups depend on factors such as infrastructure types, uncertainty consideration, and short-term impact versus long-term impact. Here, a general workflow for developing map groups is illustrated through two examples. Figure 2 shows an example workflow that creates a map group modeling flood impact on accessibility to select facilities. First, a road transportation network of the study area is constructed using graph theory. Nodes represent roadway intersection and access to select facilities. Links represent roadway links between nodes. Next, for each scenario in FPML, flood depth at road links is identified and flooded roads are removed to create an updated network. The updated network is then used to perform connectivity analysis and estimate accessibility measures. Accessibility measures (AMs) quantify flood impact on mobility. Example AMs include travel time between origin destination pairs. For additional details please refer to Panakkal et al. (2019).

Similarly, Figure 3 illustrates the methodology used for developing a probabilistic map group for residential building damage. First, obtain the building inventory and applicable probabilistic damage functions for the study area. For each flood scenario in FPML, estimate the flood depth at buildings. The flood depth at buildings is then used to estimate the probability of damage exceeding a damage state DS. P(Damage>DS) = 30% and P(Damage>DS) = 90% represent two separate maps with different confidence of damage exceeding a damage state. During emergency response, such maps can aid in optimal allocation of resources. While the example methodology showcased here utilized probabilistic damage functions for characterizing damage, a Monte-Carlo based approach can be used to quantify and propagate uncertainties associated with the building inventory and damage process.

To model the characteristics of the exposed population, map groups can be developed from available data sources such as Census data (U.S. Census Bureau 2011) and Center for Disease Control and Prevention (CDC) Social Vulnerability Index (SVI) (Flanagan et al. 2018). Some map groups such as socio-demographic data are agnostic to flood condition.

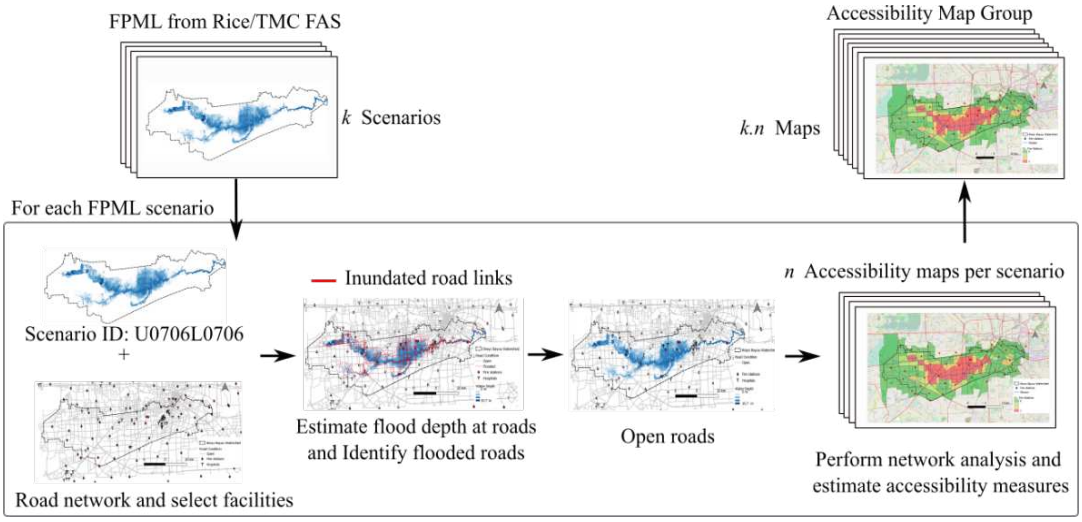

Figure 2. Methodology for developing accessibility measure map group for IPEML.

ICOSSAR 2021
The 13th International Conference on Structural Safety and Reliability (ICOSSAR 2021), June 21-25, 2021, Shanghai, P.R. China
J. Li, Pol D. Spanos, J.B. Chen & Y.B. Peng (Eds)

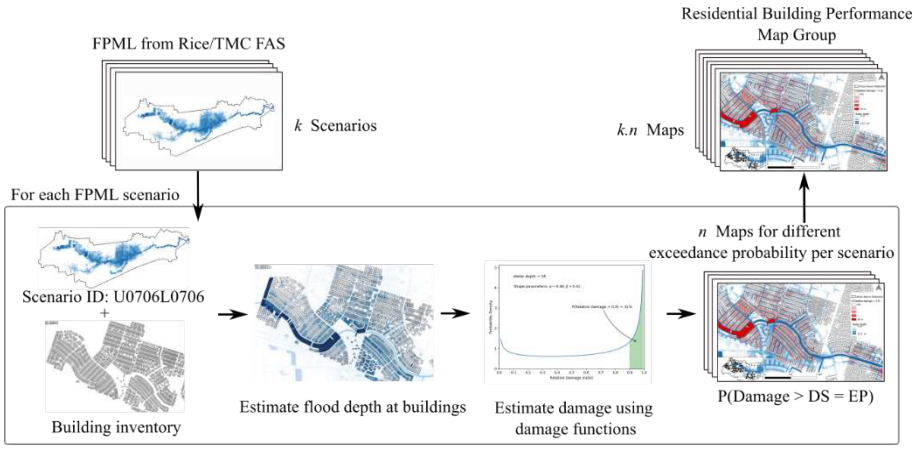

Figure 3. Methodology for developing IPEML map groups for residential building performance

2.3 *Data acquisition and map selection*

The Data Acquisition Module of RIDER acquires the current flood scenario map from Rice/TMC FAS framework at regular intervals. The current Rice/TMC FAS framework updates maps at every five-minute interval (Bedient et al. 2003). This provides sufficient temporal resolution to facilitate near-real-time decision making. Every map in the Rice/TMC FAS FPML is linked to a set of maps in IPEML using unique identifiers. For example, for an FPML scenario with ID U0706L0706, there exists at least one scenario map in all IPEML map groups. The map selection algorithm is a lookup function which selects maps from IPEML based on the current scenario ID.

2.4 *Decision-Making*

RIDER provides a query-based framework which equips a decision maker to assign weights to factors that are relevant to the evolving flood situation. The experimental framework in this study uses Python scripts in a Jupyter notebook (Kluyver et al. 2016) for user interface, GeoPandas (Jordahl 2014) for spatial queries, and Folium and Leaflet (python-visualization 2020) for visualization.

The decision-making interface provides access to pertinent spatial data from IPEML and FPML. From the list of available variables in each map, the decision maker can generate a new query or use predefined queries available in the interface. Table 1 lists example map groups and variables available from an example IPEML. Figure 4 illustrates a query. In this query, the decision maker is interested in identifying socially vulnerable census tracts which are not able to access hospitals and fire stations. Here, connectivity loss ratio of greater than 0.8 is used as a threshold for identifying regions with limited access. The mathematical expression of connectivity loss (CL) ratio is defined in Equation 1. D_{Normal} and $D_{Flooded}$ are the shortest distance between an origin-destination (OD) pair under normal and flood-affected road conditions respectively. CL ratio varies between 0 and 1 with 1 representing complete loss of access to the selected facility.

$$CL = 1 - \frac{D_{Normal}}{D_{Flooded}};\ 0 < CL \leq 1 \qquad (1)$$

Similarly, CDC SVI is used to identify vulnerable census tracts. CDC SVI quantifies social vulnerability on a 0-1 scale with higher values representing higher vulnerability. CDC estimates SVI after considering several characteristics of the population such as household composition, socioeconomic variables, race, language, ethnicity, housing, and transportation access.

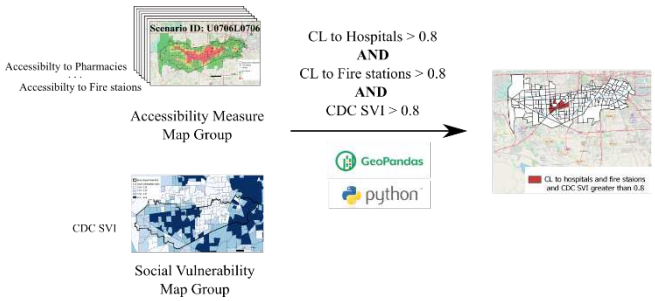

Figure 4. An example query in RIDER

ICOSSAR 2021
The 13th International Conference on Structural Safety and Reliability (ICOSSAR 2021), June 21-25, 2021, Shanghai, P.R. China
J. Li, Pol D. Spanos, J.B. Chen & Y.B. Peng (Eds)

Table 1. Map groups and available variables for an example IPEML

Map groups	Available variables
Accessibility	Accessibility measures to select facilities. Accessibility measures include connectivity loss ratio, travel time, increase in travel time compared to no flood condition, distance, increase in distance, and number of paths. Select facilities can be hospitals, fire stations, evacuation routes, pharmacies, dialysis centers, and schools.
Residential buildings	Different probability of exceeding a damage ratio.
Socio-demographic	Age, population density, education level, car ownership, language, monthly income

3 CASE STUDY APPLICATION

3.1 *Study area*

To demonstrate the application of RIDER, a case study is presented for the Brays Bayou Watershed in Houston, Texas (Fig. 5). Brays Bayou watershed is in southwest Harris County and includes a drainage area of 329 sq. km (HCFCD 2020). This densely populated watershed site several critical infrastructure facilities such as Texas Medical Center---the largest medical center in the world. In response to the widespread damage in the watershed, Rice-TMC Flood Alert system was implemented to inform emergency-response decision-making in TMC (Bedient et al. 2003). Due to the availability of Rice/TMC FAS, Brays Bayou watershed is selected for demonstrating RIDER. First, the methodology used for generating IPEML is described briefly. Then, application of the framework for a select inundation scenario from the latest FPML is presented.

3.2 *Infrastructure Performance and Exposure Map Library (IPEML)*

IPEML generated for this case study consists of three map groups. First, a deterministic map group models flood impact on the transportation network of the study area. Second, a probabilistic map group captures flood impact on residential buildings. Probabilistic damage functions from Wing et al. (2020) are used to estimate the probability of building damage exceeding a percent of its replacement value. Finally, the CDC SVI (Flanagan et al. 2018) is used to construct a socio-demographic map group.

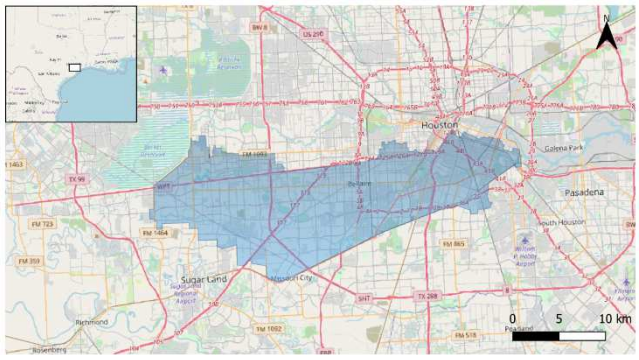

Figure 5. Location of Brays Bayou Watershed, Houston, Texas. (Source: OpenStreetMap)

Figure 2 illustrates the methodology for developing the deterministic accessibility measure map group. Road centerlines from OpenStreetMap (OpenStreetMap contributors 2017) are used to create an undirected graph network graph using NetworkX (Hagberg et al. 2008) Python library. The graph nodes represent roadway intersections and other key points such as access to select critical facilities. The selected critical facilities are hospitals and fire stations, and their locations were obtained from the Homeland Infrastructure Foundation-Level Data (HIFLD 2020) layer. The nodes are connected by links representing roadways. The network was then checked for accuracy and connectivity.

For each flood scenario in Rice/TMC FPML, a spatial overlay analysis estimates the flood depth at road links. Any road link with more than 0.60 m (2 feet) of water is assumed flooded (Gori et al. 2020). An updated network is then created by removing flooded links. Next, a network analysis estimates the accessibility measures following Panakkal et al. (2019). Figure 6 shows the road link condition for a scenario flood corresponding to seven inches of rainfall in 6 hours. The flooded roads are marked in red, and the road links, either open or outside the Brays Bayou floodplain, are

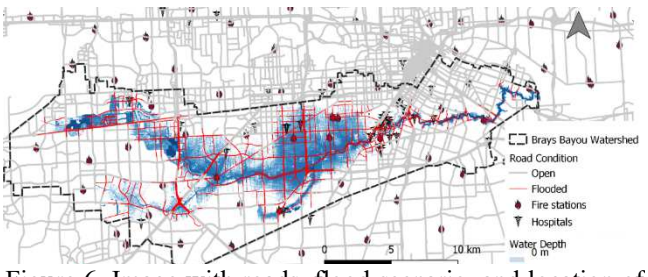

Figure 6. Image with roads, flood scenario, and location of fire stations and hospitals. Flooded roads are marked in red.

printed gray. From Figure 6, many hospitals and fire stations might be flooded in this scenario and may neither be operational nor accessible via roadways for emergency response.

Figure 7 shows the mean connectivity loss ratio between fire stations and census tracts. The mean CL ratio at a census tract is the average CL ratio of all nodes in a census tract. Regions with severely limited access to fire stations are marked red. These regions are at an elevated risk of potential secondary failures since they may not have timely access to fire stations in case of an emergency. Similarly, Figure 8 shows the flood impact on access to hospitals.

Figure 3 illustrates the methodology for developing the probabilistic residential building damage map group. The residential building inventory is obtained from the Harris County Appraisal District parcel data (HCFCD 2020). The parcel data contains information such as the number of floors and foundation type for each parcel. For each scenario in FPML, the average flood depth at parcels was estimated using spatial analysis. Flood depth inside the building can be obtained from the parcel flood depth if the building's first-floor elevation (FFE) above the ground is known. Due to the paucity of reliable FFE data, an FFE of one foot is assumed for buildings with slab foundations, and a 3 feet FFE is considered for other foundation types such as crawlspace (Gadit 2020). The water depth inside the building (i.e., average parcel flood depth - FFE) is then used to estimate flood damage to buildings.

For modeling the flood depth-damage relation, probabilistic damage functions from Wing et al. (2020) were utilized. Wing et al. proposed six depth-damage distributions for single-story residential buildings without basement using the US National Flood Insurance Program claim data. Figure 9 shows the relative damage distribution for 1.5m (5 feet) of water depth; the damage follows a Beta distribution. Similar Beta distributions are available for water depths 0.3 m (1 foot) to 1.5 m (5 feet) and 2.1 m (7 feet). Since no damage function is available if the water depth is zero or 1.8 m (6 feet), this study assumes no damage for zero water depth and uses the damage function of 2.1 m (7 feet) if the water depth is greater than 1.8 m (6 feet). This assumption could overestimate the flood damage to buildings with 1.8 m (6 feet) of water. Since the damage functions for only one-story buildings are available in Wing et al., this study only reports the damage of one-story

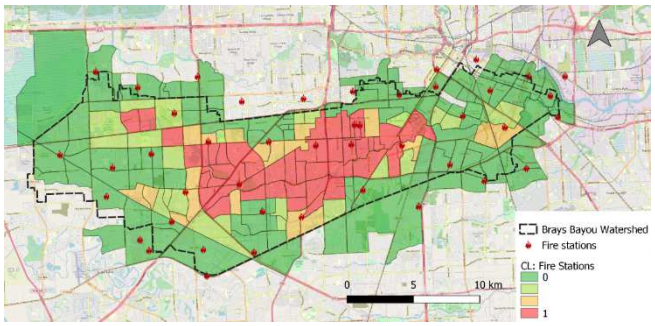

Figure 7. Flood impact on connectivity to fire stations. Census tracts with high connectivity loss ratio are marked in red

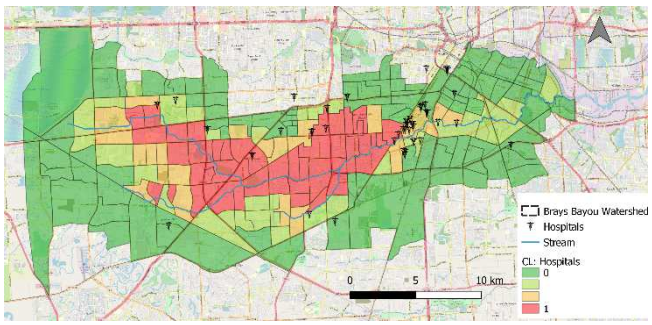

Figure 8. Flood impact on connectivity to hospitals. Census tracts with high connectivity loss ratio are marked in red

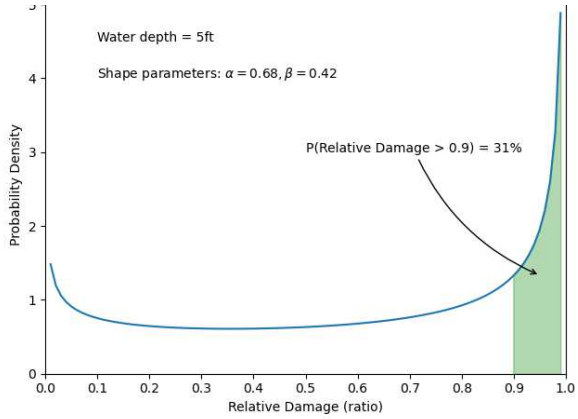

Figure 9. Probabilistic damage function for one-story residential building from Wing et al. (2020)

structures. Moreover, while developing damage functions, Wing et al. used flood claims from the entire US; this could limit the applicability of Wing et al.'s depth-damage relations to the building inventory in the Houston region. These limitations can be overcome by developing probabilistic damage functions for the study region.

For all one-story residential buildings in the Brays Bayou Watershed region, the probability of exceeding relative damage of 90 percent is

estimated from Wing et al.'s functions. The probability of exceeding 90 percent relative damage is the area highlighted in Figure 9. Relative damage is the ratio of the replacement cost to the structural value of the building. Since the functions are available only for integer water depths, the water depth at parcels is rounded to the nearest integer.

Figure 10 maps the probability of relative damage exceeding a 0.9 damage ratio for inundation scenario U0706L0706. The parcels located closer to the bayou (river) will see more significant damage than regions away from the bayou. The area located upstream of the bayou (left side in Fig. 10) will see a higher damage potential than downstream regions (right side in Fig. 10) for this scenario. While performing emergency response under limited resources, prioritizing regions with a high probability of damage exceeding a select damage state might be more impactful.

This study uses the Center for Disease Control and Prevention (CDC) Social Vulnerability Index (SVI) data for the socio-demographic map group. Figure 11 shows the spatial distribution of CDC SVI for the study region. The more vulnerable census tracts upstream might have limited access to resources to respond to and to recover from flood impacts compared to the less-vulnerable downstream census tracts.

3.3 *Decision Making*

In real-time, the RIDER framework will collect the current scenario from Rice/TMC FAS and identify the linked maps from IPEML map groups. A decision-maker can then use predefined or custom queries to gain insights. Figure 12 shows three example queries. Figure 12a highlights census tracts with CL greater than 0.8 for both fire stations and hospitals. Figure 12b highlights socially vulnerable regions with limited access to hospitals and fire stations. While Figure 12c visualizes weighted CL and SVI using equal weights, a decision-maker can combine IPEML maps using custom weights.

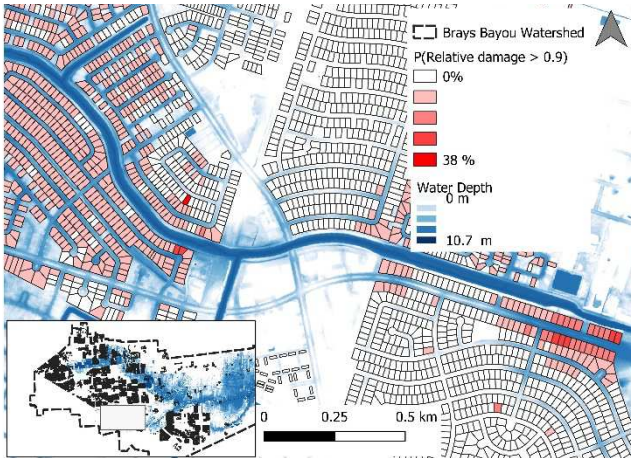

Figure 10. An example map showing the spatial distribution of residential building damage.

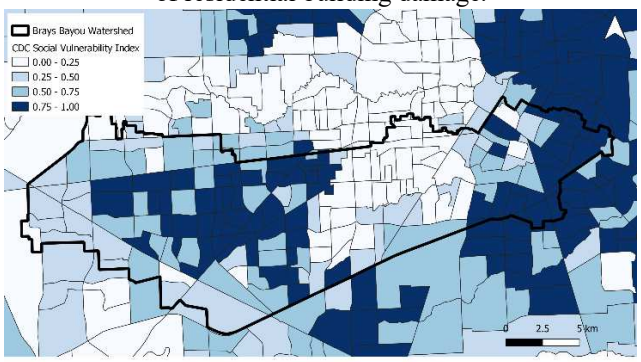

Figure 11. CDC SVI for the study area

Figure 13 illustrates a query combining CDC SVI with residential building damage. Census tract marked '1' is more socially vulnerable and contain a higher proportion of critically damaged building than the census tract marked '2'. Such spatial quantitative analysis and visualizations can

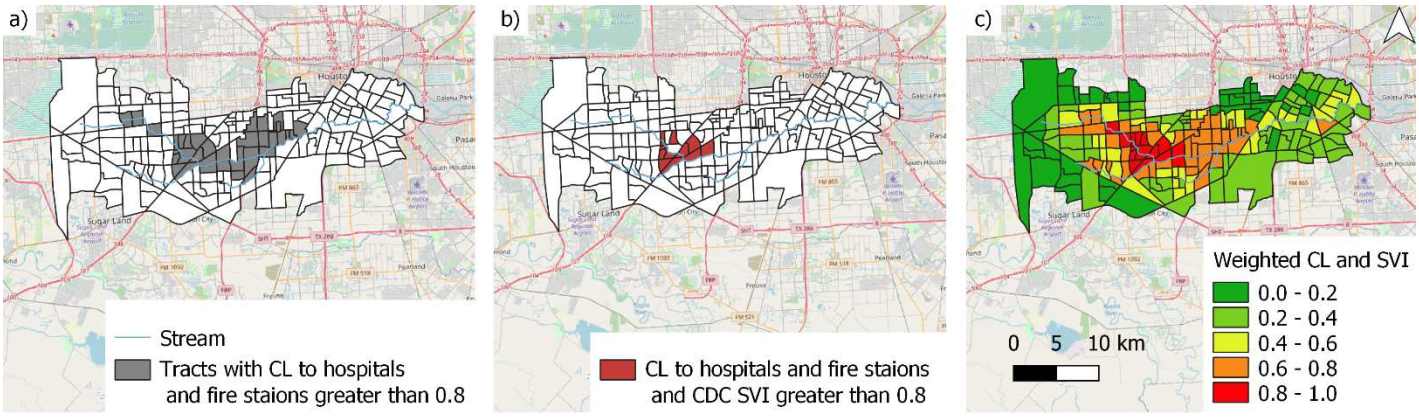

Figure 12. Example queries combining accessibility and social vulnerability.

significantly improve emergency response decision making.

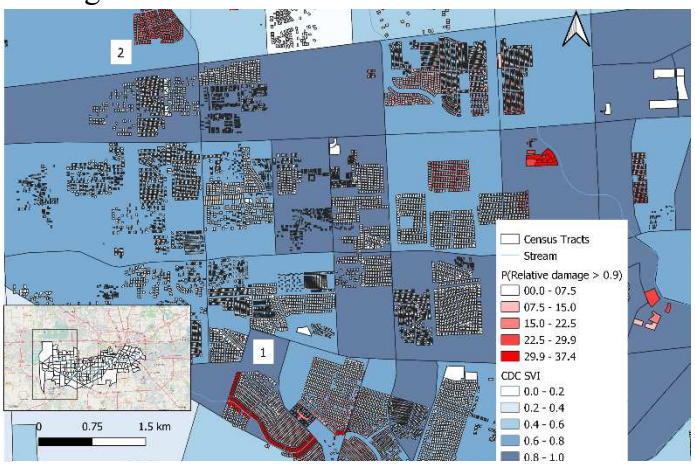

Figure 13. A query combining CDC SVI with residential building damage

4 DISCUSSION AND FUTURE WORK

This paper presents the first iteration of RIDER---a risk-informed DM framework. RIDER leverages a proven flood alert system and precompiled maps to support real-time emergency response decision-making during flooding. A case study application of RIDER to the Brays Bayou watershed, located in Houston, Texas, illustrates its capability to support decision making and potential considerations moving forward. Since the framework employs precompiled maps, it is computationally inexpensive and robust. Also, RIDER can be easily scaled to consider the flood performance of different infrastructure systems and their interactions. Moreover, RIDER facilitates risk-informed decision making by providing an efficient way to consider uncertainties either through probabilistic damage models or precompiled Monte-Carlo analyses based maps. Further, flood impacts on infrastructure systems can be placed in the context of socio-demographic data to develop a more comprehensive picture of flood consequences. In conclusion, RIDER can enhance community resilience by providing a scalable, affordable, and efficient framework to facilitate risk-informed emergency-response decision-making accessible to communities.

Although initial case studies show promising results, extensive testing and user inputs are necessary before a real-world implementation of RIDER. Also, RIDER can be further improved by a) developing probabilistic damage models for modeling flood impact on diverse infrastructure systems such as residential buildings, bridges, and industrial facilities; b) extending RIDER to also consider live data. Example live data include locations of response resources, input from structural health monitoring and Internet of Things; c) developing a web-based interface for RIDER; and d) extending RIDER to consider cumulative structural damage. To elaborate, the current iteration of RIDER does not assess cumulative structural damage to infrastructure systems through the evolution of flooding. This limitation could underestimate flood damage to infrastructure systems. Future iterations of RIDER will address these opportunities.

5 ACKNOWLEDGEMENTS

The authors gratefully acknowledge the support of this research by the National Science Foundation under awards under Smart and Connected Communities SCC-PG-1951821 and partial support from Rice University creative ventures/IDEA fund. The authors thank Xiaoyu "Toby" Li for providing the latest FPML maps for Brays Bayou. Any opinions, findings, and conclusions or recommendations expressed in this paper are those of the authors and do not necessarily reflect the views of the sponsors.

6 REFERENCES

Abdelgawad, A & Yelamarthi, K. 2016. Structural health monitoring: Internet of things application. In *2016 IEEE 59th International Midwest Symposium on Circuits and Systems (MWSCAS)*, 1-4

Balomenos, GP., Hu, Y., Padgett, JE & Shelton, K. 2019. Impact of Coastal Hazards on Residents' Spatial Accessibility to Health Services. *Journal of Infrastructure Systems* 25(4): 04019028, https://doi.org/10.1061/(ASCE)IS.1943-555X.0000509

Bedient, PB., Holder, A., Benavides, JA & Vieux, BE. 2003. Radar-Based Flood Warning System Applied to Tropical Storm Allison. *Journal of Hydrologic Engineering* 8(6): 308-18, https://doi.org/10.1061/(ASCE)1084-0699(2003)8:6(308)

Bharosa, N., Lee, J & Janssen, M. 2010. Challenges and obstacles in sharing and coordinating information during multi-agency disaster response: Propositions from field exercises. *Information Systems Frontiers* 12(1): 49-65, https://doi.org/10.1007/s10796-009-9174-z

Demir, I & Krajewski, WF. 2013. Towards an integrated Flood Information System: Centralized data access, analysis, and visualization. *Environmental Modelling &*

Software 50: 77-84, https://doi.org/10.1016/j.envsoft.2013.08.009

Fang, Z., Bedient, PB., Benavides, J & Zimmer, AL. 2008. Enhanced Radar-Based Flood Alert System and Floodplain Map Library. *Journal of Hydrologic Engineering* 13(10): 926-38, https://doi.org/10.1061/(ASCE)1084-0699(2008)13:10(926)

Fang, Z., Bedient, PB & Buzcu-Guven, B. 2011. Long-Term Performance of a Flood Alert System and Upgrade to FAS3: A Houston, Texas, Case Study. *Journal of Hydrologic Engineering* 16(10): 818-28, https://doi.org/10.1061/(ASCE)HE.1943-5584.0000374

Flanagan, BE., Hallisey, EJ., Adams, E & Lavery, A. 2018. Measuring Community Vulnerability to Natural and Anthropogenic Hazards: The Centers for Disease Control and Prevention's Social Vulnerability Index. *Journal of environmental health* 80(10): 34-36.

Gadit, M. 2020. Assessing flood mitigation strategies based on quantification of risk for economically disadvantaged watershed in houston. Rice University.

Gori, A., Gidaris, I., Elliott, JR., Padgett, J., Loughran, K., Bedient, P., Panakkal, P & Juan, A. 2020. Accessibility and Recovery Assessment of Houston's Roadway Network due to Fluvial Flooding during Hurricane Harvey. *Natural Hazards Review* 21(2): 04020005, https://doi.org/10.1061/(ASCE)NH.1527-6996.0000355

Hagberg, A., Swart, P & S Chult, D. 2008. Exploring network structure, dynamics, and function using NetworkX. Los Alamos National Lab.(LANL), Los Alamos, NM (United States).

Jiang, Y & Yuan, Y. 2019. Emergency Logistics in a Large-Scale Disaster Context: Achievements and Challenges. *International Journal of Environmental Research and Public Health* 16(5): 779, https://doi.org/10.3390/ijerph16050779

Jordahl, K. 2014. GeoPandas: Python tools for geographic data. *URL: https://github. com/geopandas/geopandas*.

Kluyver, T., Ragan-Kelley, B., Pérez, F., Granger, B., Bussonnier, M., Frederic, J., Kelley, K.,et al. 2016. Jupyter Notebooks - a publishing format for reproducible computational workflows. In *Positioning and power in academic publishing: Players, agents and agendas*, Fernando Loizides & Birgit Scmidt (eds), 87-90. Netherlands: IOS Press, <https://eprints.soton.ac.uk/403913/>

Liu, C-C., Shieh, M-C., Ke, M-S & Wang, K-H. 2018. Flood Prevention and Emergency Response System Powered by Google Earth Engine. *Remote Sensing* 10(8): 1283, https://doi.org/10.3390/rs10081283

Looper, JP & Vieux, BE. 2012. An assessment of distributed flash flood forecasting accuracy using radar and rain gauge input for a physics-based distributed hydrologic model. *Journal of Hydrology* 412-413: 114-32, https://doi.org/10.1016/j.jhydrol.2011.05.046

Panakkal, P., Juan, A., Garcia, M., Padgett, JE & Bedient, P. 2019. Towards Enhanced Response: Integration of a Flood Alert System with Road Infrastructure Performance Models. In *Structures Congress 2019: Buildings and Natural Disasters*, 294-305. American Society of Civil Engineers Reston, VA.

Perumal, T., Sulaiman, MN & Leong, CY. 2015. Internet of Things (IoT) enabled water monitoring system. In *2015 IEEE 4th Global Conference on Consumer Electronics (GCCE)*, 86-87,

Rufat, S., Tate, E., Burton, CG & Maroof, AS. 2015. Social vulnerability to floods: Review of case studies and implications for measurement. *International Journal of Disaster Risk Reduction* 14: 470-86, https://doi.org/10.1016/j.ijdrr.2015.09.013

Tokognon, CA., Gao, B., Tian, GY & Yan, Y. 2017. Structural Health Monitoring Framework Based on Internet of Things: A Survey. *IEEE Internet of Things Journal* 4(3): 619-35, https://doi.org/10.1109/JIOT.2017.2664072

Wing, OEJ., Pinter, N., Bates, PD & Kousky, C. 2020. New insights into US flood vulnerability revealed from flood insurance big data. *Nature Communications* 11(1): 1444, https://doi.org/10.1038/s41467-020-15264-2

Winsemius, HC., Aerts, JCJH., van Beek, LPH., Bierkens, MFP., Bouwman, A., Jongman, B., Kwadijk, JCJ.,et al. 2016. Global drivers of future river flood risk. *Nature Climate Change* 6(4): 381-85, https://doi.org/10.1038/nclimate2893

Zhang, W., Villarini, G., Vecchi, GA & Smith, JA. 2018. Urbanization exacerbated the rainfall and flooding caused by hurricane Harvey in Houston. *Nature* 563(7731): 384-88, https://doi.org/10.1038/s41586-018-0676-z

Zscheischler, J., Westra, S., van den Hurk, BJJM., Seneviratne, SI., Ward, PJ., Pitman, A., AghaKouchak, A.,et al. 2018. Future climate risk from compound events. *Nature Climate Change* 8(6): 469-77, https://doi.org/10.1038/s41558-018-0156-3

FEMA. 2017a. 2017 Hurricane Season FEMA After-Action Report, <https://www.fema.gov/sites/default/files/2020-08/fema_hurricane-season-after-action-report_2017.pdf> (14 January 2021).

FEMA. 2017b. Historic Disaster Response to Hurricane Harvey in Texas | FEMA.gov, 2017, <https://www.fema.gov/news-release/20200220/respuesta-historica-al-huracan-harvey-en-texas> (12 January 2021).

HCFCD. 2020. Harris County Flood Control District, 2020, <https://www.hcfcd.org/Find-Your-Watershed/Brays-Bayou> (17 January 2021).

HIFLD. 2020. Homeland Infrastructure Foundation-Level Data, 2020, <https://hifld-geoplatform.opendata.arcgis.com/> (17 January 2021).

OpenStreetMap contributors. 2017. Planet dump retrieved from https://planet.osm.org, <https://www.openstreetmap.org>

python-visualization. 2020. *Folium* (version 0.11.0), <https://python-visualization.github.io/folium/>

U.S. Census Bureau. 2011. Selected housing characteristics, <https://data.census.gov/cedsci/> (16 January 2021).

Van Ackere.,Verbeurgt.,Sloover.,Gautama.,De Wulf.,& De Maeyer. 2019. A Review of the Internet of Floods: Near Real-Time Detection of a Flood Event and Its Impact. *Water* 11(11): 2275, https://doi.org/10.3390/w11112275